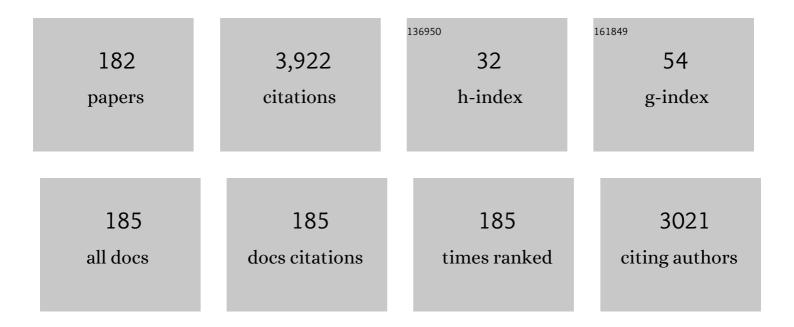
List of Publications by Year in descending order

Source: https://exaly.com/author-pdf/9511764/publications.pdf Version: 2024-02-01



TAKESHI NACASE

#	Article	IF	CITATIONS
1	Novel TiNbTaZrMo high-entropy alloys for metallic biomaterials. Scripta Materialia, 2017, 129, 65-68.	5.2	262
2	In-situ TEM observation of structural changes in nano-crystalline CoCrCuFeNi multicomponent high-entropy alloy (HEA) under fast electron irradiation by high voltage electron microscopy (HVEM). Intermetallics, 2015, 59, 32-42.	3.9	161
3	Irradiation Resistance of Multicomponent Alloys. Metallurgical and Materials Transactions A: Physical Metallurgy and Materials Science, 2014, 45, 180-183.	2.2	155
4	Development of non-equiatomic Ti-Nb-Ta-Zr-Mo high-entropy alloys for metallic biomaterials. Scripta Materialia, 2019, 172, 83-87.	5.2	124
5	Dynamic strain aging of Al 0.3 CoCrFeNi high entropy alloy single crystals. Scripta Materialia, 2015, 108, 80-83.	5.2	119
6	Microstructure of equiatomic and non-equiatomic Ti-Nb-Ta-Zr-Mo high-entropy alloys for metallic biomaterials. Journal of Alloys and Compounds, 2018, 753, 412-421.	5.5	112
7	Design and fabrication of Ti–Zr-Hf-Cr-Mo and Ti–Zr-Hf-Co-Cr-Mo high-entropy alloys as metallic biomaterials. Materials Science and Engineering C, 2020, 107, 110322.	7.3	105
8	Development of TiNbTaZrMo bio-high entropy alloy (BioHEA) super-solid solution by selective laser melting, and its improved mechanical property and biocompatibility. Scripta Materialia, 2021, 194, 113658.	5.2	95
9	Additive manufacturing of dense components in beta‑titanium alloys with crystallographic texture from a mixture of pure metallic element powders. Materials and Design, 2019, 173, 107771.	7.0	93
10	Relationship between microstrain and lattice parameter change in nanocrystalline materials. Philosophical Magazine Letters, 2008, 88, 169-179.	1.2	89
11	Formation of ultrafine-grained microstructure in Al 0.3 CoCrFeNi high entropy alloys with grain boundary precipitates. Materials Letters, 2017, 199, 120-123.	2.6	84
12	Hippo and TGF-β interplay in the lung field. American Journal of Physiology - Lung Cellular and Molecular Physiology, 2015, 309, L756-L767.	2.9	74
13	Design and development of Ti–Zr–Hf–Nb–Ta–Mo high-entropy alloys for metallic biomaterials. Materials and Design, 2021, 202, 109548.	7.0	67
14	Phase stability of amorphous and crystalline phases in melt-spun Zr66.7Cu33.3 alloy under electron irradiation. Scripta Materialia, 2003, 48, 1237-1242.	5.2	64
15	Electron-irradiation-induced structural change in Zr–Hf–Nb alloy. Intermetallics, 2012, 26, 122-130.	3.9	63
16	Effect of electron irradiation on the phase stability of Fe–9Zr–3B alloy. Materials Science & Engineering A: Structural Materials: Properties, Microstructure and Processing, 2002, 323, 218-225.	5.6	62
17	MeV electron-irradiation-induced structural change in the bcc phase of Zr–Hf–Nb alloy with an approximately equiatomic ratio. Intermetallics, 2013, 38, 70-79.	3.9	57
18	Solidification Microstructures of the Ingots Obtained by Arc Melting and Cold Crucible Levitation Melting in TiNbTaZr Medium-Entropy Alloy and TiNbTaZrX (X = V, Mo, W) High-Entropy Alloys. Entropy, 2019, 21, 483.	2.2	57

#	Article	IF	CITATIONS
19	Solidification Microstructure of AlCoCrFeNi _{2.1} Eutectic High Entropy Alloy Ingots. Materials Transactions, 2018, 59, 255-264.	1.2	56
20	Formation of nanocrystalline structure during electron irradiation induced crystallization in amorphous Fe-Zr-B alloys. Science and Technology of Advanced Materials, 2002, 3, 119-128.	6.1	53
21	Grain refinement of non-equiatomic Cr-rich CoCrFeMnNi high-entropy alloys through combination of cold rolling and precipitation of If phase. Materials Science & Engineering A: Structural Materials: Properties, Microstructure and Processing, 2018, 735, 191-200.	5.6	49
22	Temperature dependence of photoluminescence properties in a thermally activated delayed fluorescence emitter. Applied Physics Letters, 2014, 104, .	3.3	48
23	Contributions of a Higher Triplet Excited State to the Emission Properties of a Thermally Activated Delayed-Fluorescence Emitter. Physical Review Applied, 2017, 7, .	3.8	45
24	Histone methylationâ€mediated silencing of miRâ€139 enhances invasion of nonâ€smallâ€cell lung cancer. Cancer Medicine, 2015, 4, 1573-1582.	2.8	41
25	Lowâ€Temperature Processable Organicâ€Inorganic Hybrid Gate Dielectrics for Solutionâ€Based Organic Fieldâ€Effect Transistors. Advanced Materials, 2010, 22, 4706-4710.	21.0	39
26	Thermal stability and electron irradiation effect on Zr-based amorphous alloys. Journal of Applied Physics, 2003, 93, 912-918.	2.5	38
27	Electron Irradiation Induced Crystallization of the Amorphous Phase in Zr-Cu Based Metallic Glasses with Various Thermal Stability. Materials Transactions, 2004, 45, 13-23.	1.2	38
28	Formation of amorphous phase with crystalline globules in Fe–Cu–Nb–B immiscible alloys. Journal of Alloys and Compounds, 2015, 619, 267-274.	5.5	37
29	Device characteristics of short-channel polymer field-effect transistors. Applied Physics Letters, 2010, 97, .	3.3	36
30	Electron irradiation induced nano-crystallization in Zr66.7Ni33.3 amorphous alloy and Zr60Al15Ni25 metallic glass. Intermetallics, 2007, 15, 211-224.	3.9	35
31	MeV electron irradiation induced crystallization in metallic glasses: Atomic structure, crystallization mechanism and stability of an amorphous phase under the irradiation. Journal of Non-Crystalline Solids, 2012, 358, 502-518.	3.1	35
32	Multi-scale crystalline Cu globule dispersed Fe-based metallic glass formation by multi-step liquid phase separation. Journal of Alloys and Compounds, 2010, 494, 295-300.	5.5	34
33	Alloy design and fabrication of ingots in Cu-Zn-Mn-Ni-Sn high-entropy and Cu-Zn-Mn-Ni medium-entropy brasses. Materials and Design, 2019, 181, 107900.	7.0	34
34	Electron irradiation induced crystallization behavior in Zr66.7Cu33.3 and Zr65.0Al7.5Cu27.5 amorphous alloys. Materials Science & Engineering A: Structural Materials: Properties, Microstructure and Processing, 2003, 352, 251-260.	5.6	33
35	Microstructure of Ti-Ag immiscible alloys with liquid phase separation. Journal of Alloys and Compounds, 2018, 738, 440-447.	5.5	33
36	Lattice distortion and its effects on physical properties of nanostructured materials. Journal of Physics Condensed Matter, 2007, 19, 236217.	1.8	32

#	Article	IF	CITATIONS
37	Formation of amorphous phase with crystalline globules in Fe–Cu–Si–B and Fe–Cu–Zr–B immiscible alloys. Intermetallics, 2015, 61, 56-65.	3.9	32
38	Formation of Nanocrystalline Globules and Metallic Glass in Fe _{70−<1>x} Cu<1> _x Zr ₁₀ B ₂₀ (<1>x=0–70) Alloys. Materials Transactions, 2006, 47, 1105-1114.	1.2	31
39	Oxidation of Benzyl Alcohol over Nanoporous Au–CeO ₂ Catalysts Prepared from Amorphous Alloys and Effect of Alloying Au with Amorphous Alloys. Industrial & Engineering Chemistry Research, 2018, 57, 5599-5605.	3.7	30
40	Deformation behavior of HfNbTaTiZr high entropy alloy singe crystals and polycrystals. Materials Science & Engineering A: Structural Materials: Properties, Microstructure and Processing, 2021, 809, 140983.	5.6	30
41	Electron irradiation induced crystallization of the amorphous phase in Zr65.0Al7.5Ni10.0Cu17.5metallic glass. Science and Technology of Advanced Materials, 2004, 5, 57-67.	6.1	29
42	Electron irradiation-induced nanocrystallization of amorphous Fe85B15 alloy: Evidence for athermal nature. Acta Materialia, 2009, 57, 1300-1307.	7.9	28
43	Development of Ti–Zr–Hf–Y–La high-entropy alloys with dual hexagonal-close-packed structure. Scripta Materialia, 2020, 186, 242-246.	5.2	28
44	Thermal Crystallization and Electron Irradiation Induced Phase Transformation Behavior in Zr _{66.7} Cu _{33.3} Metallic Glass. Materials Transactions, 2005, 46, 616-621.	1.2	27
45	Electron Irradiation Induced Nano-Crystallization in Fe ₇₇ Nd _{4.5} B _{18.5} Metallic Glass. Materials Transactions, 2005, 46, 1814-1819.	1.2	26
46	Temperature dependence of β-phase transformation in Cu added Fe2Si5 thermoelectric material. Journal of Alloys and Compounds, 1999, 292, 181-190.	5.5	24
47	Electron Irradiation Induced Crystal-to-Amorphous-to-Crystal Transition in Some Metallic Glasses. Materials Transactions, 2007, 48, 1651-1658.	1.2	23
48	Amorphous phase formation in Fe–Ag-based immiscible alloys. Journal of Alloys and Compounds, 2015, 619, 311-318.	5.5	23
49	Solid state amorphization of metastable Al0.5TiZrPdCuNi high entropy alloy investigated by high voltage electron microscopy. Materials Chemistry and Physics, 2018, 210, 291-300.	4.0	23
50	Development of Fe-Co-Cr-Mn-Ni-C high entropy cast iron (HE cast iron) available for casting in air atmosphere. Materials and Design, 2019, 184, 108172.	7.0	23
51	Effect of rapid solidification on microstructure of various Fe29.5â^'xSi70.5â^'x (0.0≤â‰\$.7) alloys. Journal of Alloys and Compounds, 2000, 312, 295-301.	5.5	22
52	Effect of electron irradiation on nano-crystallization in Zr66.7Cu33.3 and Zr65.0Al7.5Cu27.5 amorphous alloys. Materials Science & Engineering A: Structural Materials: Properties, Microstructure and Processing, 2003, 343, 13-21.	5.6	22
53	Solid state amorphization and crystallization in Zr66.7Pd33.3 metallic glass. Intermetallics, 2006, 14, 1027-1032.	3.9	22
54	Phase Transformation in Fe81.0Zr9.0B10.0 Metallic Glass during Thermal Annealing and Electron Irradiation. ISIJ International, 2006, 46, 1371-1380.	1.4	22

#	Article	IF	CITATIONS
55	Design and microstructure analysis of globules in Al-Co-La-Pb immiscible alloys with an amorphous phase. Materials and Design, 2017, 117, 338-345.	7.0	22
56	In situ TEM observation of the glass-to-liquid transition of metallic glass in Fe–Zr–B–Cu alloy. Scripta Materialia, 2010, 63, 1020-1023.	5.2	20
57	Effect of two-stage deformation on magnetic properties of hot-deformed Nd–Fe–B permanent magnets. Scripta Materialia, 2014, 78-79, 37-40.	5.2	20
58	Formation of nanoglobules with core–shell structure by liquid phase separation in Fe–Cu–Zr–B immiscible alloy. Journal of Alloys and Compounds, 2015, 619, 332-337.	5.5	20
59	Effect of irradiation temperature on the electron irradiation induced nanocrystallization behavior in Fe88.0Zr9.0B3.0 amorphous alloy. Materials Science & Engineering A: Structural Materials: Properties, Microstructure and Processing, 2003, 347, 136-144.	5.6	19
60	Electron-irradiation-induced nano-crystallization in quasicrystal-forming Zr-based metallic glass. Intermetallics, 2009, 17, 657-668.	3.9	19
61	Stability of B2 phase in Ti–Ni–Fe alloys against MeV electron-irradiation-induced solid-state amorphization and martensite transformation. Intermetallics, 2011, 19, 1313-1318.	3.9	19
62	Electron irradiation induced phase transformation in Zr66.7Cu33.3 and Zr66.7Pd33.3 metallic glass. Scripta Materialia, 2005, 53, 1401-1405.	5.2	18
63	Preparation of Zr-Based Metallic Glass Wires for Biomaterials by Arc-Melting Type Melt-Extraction Method. Materials Transactions, 2008, 49, 1385-1394.	1.2	18
64	Formation of macroscopically phase separated Cu-colored melt-spun ribbon in (Fe0.5Cu0.5)100â^'B (x= 0,) Tj E	[Qq0 0 0 r 5.5	gBT /Overlock
65	Formation of melt-extracted wire of Fe–Cu–Si–B alloy with core-wire/surface-cover-layer structure by arc-melt-type melt-extraction method. Journal of Alloys and Compounds, 2010, 495, L1-L4.	5.5	17
66	Electron-Irradiation Induced Phase Transformation of Amorphous, Supercooled Liquid and Crystalline Phases in Zr _{66.7} Cu _{33.3} Metallic Glass. Materials Transactions, 2006, 47, 1469-1479.	1.2	16
67	Stability of oxide particles under electron irradiation in a 9Cr ODS steel at 400 °C. Journal of Nuclear Materials, 2014, 455, 724-727.	2.7	16
68	Amorphous phase formation in Co–Cu–Zr–B-based immiscible alloys. Journal of Alloys and Compounds, 2015, 649, 1174-1181.	5.5	16
69	Determination of deep trapping lifetime in organic semiconductors using impedance spectroscopy. Applied Physics Letters, 2016, 108, 053305.	3.3	16
70	Formation of dual-layer melt-spun ribbon through liquid phase separation. Intermetallics, 2010, 18, 2136-2144.	3.9	15
71	Skeletal Ni Catalysts Prepared from Amorphous Ni–Zr Alloys: Enhanced Catalytic Performance for Hydrogen Generation from Ammonia Borane. ChemPhysChem, 2016, 17, 412-417.	2.1	15
72	Alloy Design and Fabrication of Ingots of Al–Mg–Li–Ca Light-Weight Medium Entropy Alloys. Materials Transactions, 2020, 61, 1369-1380.	1.2	15

#	Article	IF	CITATIONS
73	Effect of crystallization behavior on the oxidation resistance of a Zr–Al–Cu metallic glass below the crystallization temperature. Journal of Non-Crystalline Solids, 2006, 352, 3015-3026.	3.1	14
74	Electron Irradiation–Induced Phase Transition of an Amorphous Phase and Face-Centered Cubic Solid Solutions in Zr66.7Pd33.3 Metallic Glass. Metallurgical and Materials Transactions A: Physical Metallurgy and Materials Science, 2007, 38, 223-235.	2.2	14
75	Liquid Phase Separation in Ag-Co-Cr-Fe-Mn-Ni, Co Cr-Cu-Fe-Mn-Ni and Co-Cr-Cu-Fe-Mn-Ni-B High Entropy Alloys for Biomedical Application. Crystals, 2020, 10, 527.	2.2	14
76	Interleukin-17A and Toll-Like Receptor 3 Ligand Poly(I:C) Synergistically Induced Neutrophil Chemoattractant Production by Bronchial Epithelial Cells. PLoS ONE, 2015, 10, e0141746.	2.5	14
77	Electron Irradiation Induced Nanocrystallization Behavior in Fe ₇₁ Zr ₉ B ₂₀ Metallic Glass. Materials Transactions, 2005, 46, 608-615.	1.2	13
78	Temperature dependence in density-fluctuation-induced crystallization in metallic glass by MeV electron irradiation. Intermetallics, 2010, 18, 1803-1808.	3.9	13
79	Synthesis of metal silicide at metal/silicon oxide interface by electronic excitation. Journal of Applied Physics, 2015, 117, .	2.5	13
80	Development of Co–Cr–Mo–Fe–Mn–W and Co–Cr–Mo–Fe–Mn–W–Ag High-Entropy Al Co–Cr–Mo Alloys. Materials Transactions, 2020, 61, 567-576.	oys Based	on 13
81	Eutectoid decomposition in rapidly solidified α-Fe2Si5-based thermoelectric alloys. Journal of Alloys and Compounds, 2001, 316, 212-219.	5.5	12
82	Phase stability in nanocrystalline metals: A thermodynamic consideration. Journal of Applied Physics, 2007, 102, 124303.	2.5	12
83	Electron-irradiation-induced solid-state amorphization caused by thermal relaxation of lattice defects. Intermetallics, 2010, 18, 441-450.	3.9	12
84	Tensile deformation behavior of Nd–Fe–B alloys. Scripta Materialia, 2011, 65, 743-746.	5.2	12
85	Ti- and Zr-based metal-air batteries. Journal of Power Sources, 2013, 242, 400-404.	7.8	12
86	Phase stability of σ-CrFe intermetallic compound under fast electron irradiation. Acta Materialia, 2014, 71, 195-205.	7.9	12
87	Skeletal Au prepared from Au–Zr amorphous alloys with controlled atomic compositions and arrangement for active oxidation of benzyl alcohol. Journal of Materials Chemistry A, 2016, 4, 8458-8465.	10.3	12
88	Electron irradiation induced crystallization and amorphization in Fe77Nd4.5B18.5 metallic glass. Materials Science & Engineering A: Structural Materials: Properties, Microstructure and Processing, 2007, 449-451, 1115-1118.	5.6	11
89	Electron Irradiation Induced Phase Transformation in Fe-Nd-B Alloys. Materials Transactions, 2007, 48, 1659-1664.	1.2	10
90	Preparation of Ni–Nb-based metallic glass wires by arc-melt-type melt-extraction method. Journal of Alloys and Compounds, 2009, 485, 304-312.	5.5	10

6

#	Article	IF	CITATIONS
91	Electron-irradiation-induced solid-state amorphization in supersaturated Ni–Zr solid solutions. Intermetallics, 2011, 19, 511-517.	3.9	10
92	Mechanism of instability of carbides in Fe–TaC alloy under high energy electron irradiation at 673 K. Journal of Nuclear Materials, 2014, 455, 695-699.	2.7	10
93	New Approach to <i>In Situ</i> Observation Experiments under Irradiation in High Voltage Electron Microscopes. Materials Transactions, 2014, 55, 423-427.	1.2	10
94	Formation of macroscopic phase-separated dual-layer melt-spun ribbon from Co–Si–B–Cu alloy. Journal of Alloys and Compounds, 2010, 505, L43-L46.	5.5	9
95	Effect of Ni-addition on the crystallization behavior and the oxidation resistance of Zr-based metallic glasses below the crystallization temperature. Journal of Non-Crystalline Solids, 2011, 357, 1136-1140.	3.1	9
96	Electron-irradiation-induced phase transition in Cr2M (M = Ti and Al) intermetallic compounds. Journal of Alloys and Compounds, 2013, 579, 646-653.	5.5	9
97	Microstructure of Rapidly Solidified Fe-M-Si-B (M=Cu, Ag, Sn) Immiscible Alloys. Zairyo/Journal of the Society of Materials Science, Japan, 2015, 64, 175-182.	0.2	9
98	Microstructure and Magnetic Properties of Cu–Ag–La–Fe Immiscible Alloys with an Amorphous Phase. Materials Transactions, 2019, 60, 554-560.	1.2	9
99	Design and development of (Ti, Zr, Hf)-Al based medium entropy alloys and high entropy alloys. Materials Chemistry and Physics, 2022, 276, 125409.	4.0	9
100	Title is missing!. Journal of Materials Science, 2002, 37, 1429-1435.	3.7	8
101	é‡'å±žææ–™ã«ãŠã'ā,‹é›»åç·šç§å°"èª~起相転移. Materia Japan, 2008, 47, 519-523.	0.1	8
102	Solution-processed dinaphtho[2,3- <i>b</i> :2′,3′- <i>f</i>]thieno[3,2- <i>b</i>]thiophene transistor memory based on phosphorus-doped silicon nanoparticles as a nano-floating gate. Applied Physics Express, 2015, 8, 101601.	2.4	8
103	Microstructure of rapidly solidified Co–Cu–Si–B immiscible alloys with an amorphous phase. Journal of Alloys and Compounds, 2015, 650, 342-350.	5.5	8
104	Microstructure of Co-Cr-Fe-Mn-Ni-Cu and Co-Cr-Fe-Mn-Ni-Ag High Entropy Alloys with Liquid Phase Separation. Materials Science Forum, 2018, 941, 1238-1241.	0.3	8
105	Phase Stability of an Amorphous Phase Against Electron Irradiation Induced Crystallization in Fe-Based Metallic Glasses. Materials Transactions, 2007, 48, 1340-1349.	1.2	7
106	Fabrication of Ti-Zr Binary Metallic Wire by Arc-Melt-Type Melt-Extraction Method. Materials Transactions, 2009, 50, 872-878.	1.2	7
107	Dynamic Observation of FeSiBPCu Alloys for Crystallization via MeV Electron Irradiation. Nippon Kinzoku Gakkaishi/Journal of the Japan Institute of Metals, 2014, 78, 364-368.	0.4	7
108	Prediction of improvement in left atrial function index after catheter ablation for atrial fibrillation. Journal of Interventional Cardiac Electrophysiology, 2015, 44, 151-160.	1.3	7

#	Article	IF	CITATIONS
109	Hydrogenation of 1-octene over skeletal Pd catalysts prepared from Pd–Zr amorphous alloys and the effect of Ni addition. Catalysis Today, 2016, 265, 138-143.	4.4	7
110	Long period structure of Î ² -FeSi2. Journal of Alloys and Compounds, 2002, 339, 96-99.	5.5	6
111	Transformation Behavior of TiNiPt Thin Films Fabricated Using Melt Spinning Technique. Materials Research Society Symposia Proceedings, 2004, 842, 144.	0.1	6
112	Electron Irradiation Induced Phase Transformation in Nd ₂ Fe ₁₄ B Alloy. Materials Transactions, 2006, 47, 1762-1768.	1.2	6
113	Martensitic Transformation Behavior and Shape Memory Properties of Ti–Ni–Pt Melt-Spun Ribbons. Materials Transactions, 2006, 47, 540-545.	1.2	6
114	Electron Irradiation Induced Crystallization Behavior in Zr _{66.7} M _{33.3} (M=Cu,) Tj ETQ	999.90 rg	3T /Overlock
115	In situ observation of solid-state amorphization in Nd2Fe14B alloy by electron irradiation. Materials Science & Engineering A: Structural Materials: Properties, Microstructure and Processing, 2007, 449-451, 1111-1114.	5.6	6
116	In situ TEM observations of irradiation-induced phase change in tungsten. Journal of Materials Science, 2009, 44, 1965-1968.	3.7	6
117	Temperature dependence of MeV-electron-irradiation-induced nanocrystallization in Zr–Pt metallic glass. Intermetallics, 2010, 18, 767-772.	3.9	6
118	Entangled Duplex Structure and Polycrystalline Globule Formation through Multistep Liquid-Phase Separation in Cu–Fe–Zr–B Alloys. Materials Transactions, 2014, 55, 304-310.	1.2	6
119	<i>Pseudomonas aeruginosa</i> quorum-sensing signaling molecule N-3-oxododecanoyl homoserine lactone induces matrix metalloproteinase 9 expression via the AP1 pathway in rat fibroblasts. Bioscience, Biotechnology and Biochemistry, 2015, 79, 1719-1724.	1.3	6
120	Fabrication of the Beta-Titanium Alloy Rods from a Mixture of Pure Metallic Element Powders via Selected Laser Melting. Materials Science Forum, 0, 941, 1260-1263.	0.3	6
121	Solidification Microstructure of High Entropy Alloys Composed With 4 Group (Ti, Zr, Hf), 5 Group (V,) Tj ETQq1 1	0.784314	rgBT /Over
122	Control of a Nanocomposite Structure in Fe ₈₆ Nd ₉ B ₅ Alloy by Electron Irradiation. Materials Transactions, 2006, 47, 335-340.	1.2	5
123	Synthesis of refractory conductive niobium carbide nanowires within the inner space of carbon nanotube templates. Applied Physics Express, 2014, 7, 015101.	2.4	5
124	Characteristics and Catheter Ablation of Focal Atrial Tachycardia Originating From the Interatrial Septum. Heart Lung and Circulation, 2015, 24, 988-995.	0.4	5
125	Formation of Various Types of Globules in Co–Cu–Si–B Immiscible Alloy with Amorphous Phase. Materials Transactions, 2016, 57, 156-162.	1.2	5
126	Microstructure of nanocrystalline globules embedded in an amorphous matrix of Fe–Cuâ€based immiscible alloys. Surface and Interface Analysis, 2016, 48, 1252-1255.	1.8	5

#	Article	IF	CITATIONS
127	Solidification Microstructure and Magnetic Properties of Ag-Rich Ag–Cu–La–Fe Immiscible Alloys. Materials Transactions, 2020, 61, 311-317.	1.2	5
128	Advanced Materials Design by Irradiation of High Energy Particles. , 2013, , 137-153.		5
129	Electron irradiation induced phase transformation of supercooled liquid and amorphous phases in Zr66.7Cu33.3 metallic glass. Materials Science & Engineering A: Structural Materials: Properties, Microstructure and Processing, 2007, 449-451, 605-608.	5.6	4
130	Microstructure observation using MeV-electron-irradiation-induced amorphization. Journal of Alloys and Compounds, 2011, 509, S202-S205.	5.5	4
131	Electron-irradiation-induced crystallization at metallic amorphous/silicon oxide interfaces caused by electronic excitation. Journal of Applied Physics, 2016, 119, .	2.5	4
132	Microstructure and Magnetic Properties of Cu-Ag-La-Fe Immiscible Alloys with an Amorphous Phase. Funtai Oyobi Fummatsu Yakin/Journal of the Japan Society of Powder and Powder Metallurgy, 2018, 65, 45-51.	0.2	4
133	Solidification Microstructure and Magnetic Properties of Ag-rich Ag-Cu-La-Fe Immiscible Alloys. Zairyo/Journal of the Society of Materials Science, Japan, 2019, 68, 205-211.	0.2	4
134	Effect of Chemical Composition on Grain Refinement of Al _x CoCrFeNi High Entropy Alloys with NiAl Grain Boundary Precipitates. Materials Science Forum, 0, 1016, 1690-1695.	0.3	4
135	PM-09Microstructure of Ti-Nb-Ag Immiscible Alloys with Liquid Phase Separation. Microscopy (Oxford,) Tj ETQq1	1 0.78431 1.5	.4 ₄ gBT /Ovei
136	Electron Irradiation Induced Amorphization and Crystallization in Zr _{66.7} Cu _{33.3} Metallic Glass. Journal of Metastable and Nanocrystalline Materials, 2005, 24-25, 661-664.	0.1	3
137	Effect of Electron Irradiation on Nanocrystallization of Fe-Nd-B Amorphous Alloys. Materials Science Forum, 2006, 512, 107-110.	0.3	3
138	Nano-Crystallization and Stability of an Amorphous Phase in Fe-Nd-B Alloy under 2.0 MeV Electron Irradiation. Materials Transactions, 2008, 49, 265-274.	1.2	3
139	Solid-state amorphization in a Ti2Pd intermetallic compound under fast-electron irradiation. Journal of Alloys and Compounds, 2013, 581, 324-329.	5.5	3
140	Temperature Dependence of Field-Effect Mobility in Organic Thin-Film Transistors: Similarity to Inorganic Transistors. Journal of Nanoscience and Nanotechnology, 2016, 16, 3219-3222.	0.9	3
141	Microstructure of Rapidly Solidified Melt-Spun Ribbon in AlCoCrFeNi _{2.1} Eutectic High-Entropy Alloys. Materials Science Forum, 0, 879, 1350-1354.	0.3	3
142	In situ transmission-electron-microscopy observation of solid-state amorphization behavior in Ti50Ni44Fe6 alloy by high-voltage electron microscopy. Acta Materialia, 2016, 104, 201-209.	7.9	3
143	Fabrication of the Casting Products in Cu–Zn–Mn–Ni Medium-Entropy Brasses. Materials Transactions, 2021, 62, 856-863.	1.2	3
144	Development of Fe–P–C–Cu Immiscible Amorphous Alloys with Liquid Phase Separation. ISIJ International, 2020, 60, 2615-2624.	1.4	3

#	Article	IF	CITATIONS
145	Deformation behavior of Zr60.0Al15.0Ni25.0 metallic glass. Intermetallics, 2006, 14, 1079-1084.	3.9	2
146	Superplastic Deformation and Thermal Crystallization Behavior of Supercooled Liquid in Zr-Ni Based Metallic Glass. Materials Science Forum, 2006, 512, 37-40.	0.3	2
147	Electron Irradiation Induced Crystallization of Supercooled Liquid in Zr Based Alloys. Materials Transactions, 2007, 48, 151-157.	1.2	2
148	Electron Irradiation Induced Crystal-to-Amorphous-to-Crystal (C-A-C) Transition in Intermetallic Compounds. Materials Research Society Symposia Proceedings, 2008, 1128, 54901.	0.1	2
149	Amorphization and subsequent crystallization in Zr66.7Ni33.3alloy under MeV electron irradiation. Journal of Physics: Conference Series, 2009, 165, 012075.	0.4	2
150	An amorphous phase formation at palladium / silicon oxide (Pd/SiOx) interface through electron irradiation - electronic excitation process. AIP Advances, 2015, 5, 117145.	1.3	2
151	An Amorphous Phase Formation in Co-Cu-Zr-Ti-B Alloy System. Funtai Oyobi Fummatsu Yakin/Journal of the Japan Society of Powder and Powder Metallurgy, 2016, 63, 217-222.	0.2	2
152	Alloy Design, Thermodynamics, and Electron Microscopy of Ternary Ti-Ag-Nb Alloy with Liquid Phase Separation. Materials, 2020, 13, 5268.	2.9	2
153	MeV Electron Irradiation Induced Solid-State Amorphization (SSA) in B2 Intermetallic Compounds. Zairyo/Journal of the Society of Materials Science, Japan, 2013, 62, 185-190.	0.2	2
154	Electron Microscopy on Cu Element Distribution in Spheroidal Graphite Cast Iron. Materials Transactions, 2020, 61, 1853-1861.	1.2	2
155	Relationship between Deformation and Crystallization in Zr ₆₀ Al ₁₅ Ni ₂₅ and Zr ₆₅ Al _{7.5} Cu _{27.5} Metallic Glass. Materials Transactions, 2005, 46, 2908-2914.	1.2	1
156	Phase Transformation and Microstructure Change in Fe-Zr-B Amorphous Alloys by Thermal Annealing and Electron Irradiation. Journal of Metastable and Nanocrystalline Materials, 2005, 24-25, 295-298.	0.1	1
157	Pinpoint Nano-Crystallization and Magnetization in Fe-Nd-B Metallic Glass by Electron Irradiation. Materials Science Forum, 2007, 561-565, 1403-1406.	0.3	1
158	Preparation of Zr-based Metallic Glass Wire for Biomedical Application. Materials Research Society Symposia Proceedings, 2007, 1048, 13.	0.1	1
159	Microstructual Observation by Use of the Difference in the Susceptibility to C-A Transition under MeV Electron Irradiation. Materia Japan, 2009, 48, 607-607.	0.1	1
160	Ultra High Voltage Electron Microscopy Study of {113}-Defect Generation in Si Nanowires. Materials Research Society Symposia Proceedings, 2014, 1713, 1.	0.1	1
161	Irradiation damage in multicomponent equimolar alloys and high entropy alloys (HEAs). Microscopy (Oxford, England), 2014, 63, i22.2-i22.	1.5	1
162	Impact of dopants and silicon structure dimensions on {113}-defect formation during 2 MeV electron irradiation in an UHVEM. Physica Status Solidi C: Current Topics in Solid State Physics, 2015, 12, 1160-1165.	0.8	1

#	Article	IF	CITATIONS
163	In situ UHVEM irradiation study of intrinsic point defect behavior in Si nanowire structures. Physica Status Solidi C: Current Topics in Solid State Physics, 2015, 12, 275-281.	0.8	1
164	PM-01Electron-Irradiation-Induced Structural Changes at Pt/SiO _x Interfaces at 773 K. Microscopy (Oxford, England), 2016, 65, i32.1-i32.	1.5	1
165	In situ atomic-level observation of the formation of platinum silicide at platinum-silicon oxide interfaces under electron irradiation. AIP Advances, 2018, 8, 055110.	1.3	1
166	Scanning Transmission Electron Microscopy (STEM) Observation of the Nuclei in Spheroidal Graphite Cast Iron. Materia Japan, 2019, 58, 86-86.	0.1	1
167	Development and Perspectives of High Entropy alloys composed by light metal elements and that for metallic biomaterials with BCC. Keikinzoku/Journal of Japan Institute of Light Metals, 2020, 70, 14-23.	0.4	1
168	Martensitic Transformation Behavior and Shape Memory Properties of Ti-Ni-Pt Melt Spun Ribbon. Nippon Kinzoku Gakkaishi/Journal of the Japan Institute of Metals, 2005, 69, 628-633.	0.4	0
169	Unique Nano-Crystalline Structure Formation in Zr-Pd Metallic Glass by Electron Irradiation Technique. Materials Science Forum, 2007, 561-565, 1407-1412.	0.3	0
170	Phase Stability of Crystalline and Amorphous Phases and Formation of Nanostructure in Zr-Pd and Zr-Pt Alloys Under Electron Irradiation. Materials Research Society Symposia Proceedings, 2007, 1048, 3.	0.1	0
171	Control of Nano-crystalline Structure in Fe-Nd-B Metallic Glass by MeV Electron Irradiation Induced Crystallization. Materia Japan, 2010, 49, 323-324.	0.1	0
172	Structure and Mechanical Properties of Melt-Extracted Beta-Ti-Type Ti-Nb-Ta-Zr (TNTZ) Wire with High Bending Ductility. Nippon Kinzoku Gakkaishi/Journal of the Japan Institute of Metals, 2010, 74, 515-519.	0.4	0
173	Fabrication of Beta-Ti-Type Ti-Nb-Ta-Zr (TNTZ) Wire with High-Ductility by Arc-Melt-Type Melt-Extraction Method. Materials Transactions, 2010, 51, 377-380.	1.2	0
174	Preparation of Ti-Based and Zr-Based Bio-Metallic Wires by Arc-Melting Type Melt-Extraction Method. Materials Science Forum, 2010, 638-642, 2127-2132.	0.3	0
175	<i>In Situ</i> TEM Observation of Structural Changes in Rapidly Solidified bcc Solid-Solution Phase in Ti–Cr Alloy Focusing on Spontaneous Vitrification (SV). Materials Transactions, 2014, 55, 451-457.	1.2	0
176	Irradiation-induced ordering in Pt-Cu alloy focusing on Pt7Cu. Materials Research Society Symposia Proceedings, 2015, 1760, 114.	0.1	0
177	Phase transition of sigma-CrFe under fast electron irradiation. Materials Research Society Symposia Proceedings, 2015, 1743, 64.	0.1	0
178	3aA_MI-1Nuclei of BCC Phase in AlTi0.5ZrCuNiPd High Entropy Alloy. Microscopy (Oxford, England), 2018, 67, i25-i25.	1.5	0
179	Fabrication of Be-Ta Ti Alloys without Pre-Alloyed Powders via SLM. Materials Science Forum, 0, 1016, 1797-1801.	0.3	0
180	Solid State Amorphization and Alloy Parameters for High Entropy Alloys. Materials Science Forum, 0, 1016, 990-996.	0.3	0

#	Article	IF	CITATIONS
181	Electron Irradiation Induced Crystal-to-amorphous-to-crystal (C-A-C) Transition. Materia Japan, 2008, 47, 644-644.	0.1	0
182	The Formation of a Glass. Zairyo/Journal of the Society of Materials Science, Japan, 2017, 66, 251-252.	0.2	0